Influence of formulation parameters on the physicochemical properties of meloxicam-loaded solid lipid nanoparticles

Rawia M. Khalil[a], Ahmed Abd El-Bary[b], Mahfoz A. Kassem[a], Mamdouh M. Ghorab[c] and Mona Basha[a]

[a]Department of Pharmaceutical Technology, National Research Centre, [b]Department of Pharmaceutics, Faculty of Pharmacy, Cairo University, Cairo and [c]Department of Pharmaceutics, Faculty of Pharmacy, Suez Canal University, Ismailia, Egypt

Correspondence to Rawia M. Khalil, Department of Pharmaceutical Technology, National Research Centre, El-Bohowth St., PO Box 12622, Dokki, 12311 Cairo, Egypt
Tel: +20 1006935895/+1006550825;
fax: +20 233370931;
e-mail: rawia_khalil@yahoo.com

Received 26 November 2012
Accepted 4 February 2013

Egyptian Pharmaceutical Journal
2013, 12:63–72

Objective
The aim of this research was to investigate novel particulate carrier systems such as solid lipid nanoparticles (SLNs) for topical delivery of a lipophilic drug, meloxicam (MLX).

Methods
MLX-loaded SLNs were prepared using a modified high-shear homogenization and ultrasonication technique using different types of lipids and surfactants. Lipid nanoparticles were characterized in terms of entrapment efficiency, particle size, Zeta potential, differential scanning calorimetry, transmission electron microscopy, and in-vitro release studies.

Results
The lipid nanoparticles showed mean diameters of 210–730 nm, whereas the entrapment efficiency ranged from 50 to 84% depending on emulsifier and lipid concentration or type. MLX-loaded SLNs showed spherical particles with Zeta potentials varying from −15.7 to −30.5 mV. A differential scanning calorimetry study revealed that MLX encapsulated in SLNs was in the amorphous form. All nanoparticle formulations exhibited sustained release characteristics, and the release pattern followed the Higuchi's equation. The analysis of results revealed that the type and concentration of the emulsifier or lipid used had a significant effect on the physicochemical properties on the investigated SLNs formulations.

Conclusion
The present study indicates that SLNs could potentially be exploited as carrier systems for MLX, with improved drug loading capacity and controlled drug release.

Keywords:
differential scanning calorimetry, in-vitro release study, meloxicam, solid lipid nanoparticles, topical delivery

Egypt Pharm J 12:63–72

1687-4315

Introduction

In recent years, significant effort has been devoted to develop nanotechnology for drug delivery. Solid lipid nanoparticles (SLNs) are aqueous colloidal dispersions, the matrix of which comprises solid biodegradable lipids. SLNs combine the advantages and avoid the drawbacks of several colloidal carriers of their class such as physical stability, protection of incorporated labile drugs from degradation, controlled release, and excellent tolerability [1]. SLNs offer a suitable means of delivering drugs for various application routes; they attract great attention as novel colloidal drug carriers for topical use [2]. The advantages of these carriers include negligible skin irritation, controlled release, and protection of active substances [3]. Because they are composed of nonirritative and nontoxic lipids, SLNs seem to be well suited for use on inflamed and damaged skin. Moreover, SLNs have distinct occlusive properties because of the formation of an intact film on the skin surface upon drying, which decreases transepidermal water loss and favors drug penetration through the stratum corneum [4]. Besides having a highly specific surface area, nanometer-sized SLNs also facilitate the contact of the encapsulated drug with the stratum corneum [4]. The nanometer-sized particles can make close contact with superficial junctions of corneocyte clusters and furrows between corneocyte islands, which may favor accumulation for several hours, allowing for sustained drug release [5]. Other advantages of SLNs include a high drug payload and incorporation of lipophilic and hydrophilic drugs [2]. SLNs have been used to improve skin/dermal uptake of several drugs [6,7], which supports the idea that SLNs can be used as carriers for topical delivery of meloxicam (MLX).

MLX is a potent, nonsteroidal anti-inflammatory water-insoluble drug [8,9]. It inhibits cyclooxygenase (COX). MLX is more selective for the COX-2 isoform of prostaglandin synthetase compared with the COX-1 form. Therefore, MLX has been labeled a 'preferential' inhibitor instead of a 'selective' inhibitor of COX-2 [10].

1687-4315 © 2013 Division of Pharmaceutical and Drug Industries Research, National Research Centre DOI: 10.7123/01.EPJ.0000428643.74323.d9

The intention of this study was to prepare and evaluate MLX-loaded SLNs and to optimize the formulation parameters in order to fabricate SLN dispersions of desired characteristics for topical delivery of MLX, aiming to improve skin uptake and reduce systemic absorption and dermal irritation.

Materials and methods

Materials

MLX was supplied by Medical Union Pharmaceuticals (Ismailia, Egypt). Geleol (glyceryl monostearate 40–55; 40–55% monoglycerides, 30–45% diglycerides, melting point (m.p.) 54.5–58.5°C), Compritol 888 ATO (glyceryl behenate; 15–23% monoglycerides, 40–60% diglycerides, 21–35% triglycerides, m.p. 69.0–74.0°C), and Precirol ATO5 (glyceryl palmitostearate; 8–22% monoglycerides, 40–60% diglycerides, 25–35% triglycerides, m.p. 50–60°C) were kindly donated by Gattefossé (Saint-Priest, France). Tween 80 (polysorbate 80), methanol Chromasolv, and dialysis tubing cellulose membrane (molecular weight cutoff 12 000 g/mole) were purchased from Sigma Chemical Company (St. Louis, Missouri, USA). Cremophor RH40 (polyoxyl 40 hydrogenated castor oil) was kindly donated by BASF (Ludwigshafen, Germany). All other chemicals and reagents used were of analytical grade.

Methods

Preparation of solid lipid nanoparticles

SLNs were prepared by a slight modification of the previously reported high-shear homogenization and ultrasonication technique [11,12]. Briefly, the lipid phase consisted of Geleol, Compritol, or Precirol as the solid lipid was melted 5°C above the melting point of the lipid used. MLX (0.5%w/w) was dissolved therein to obtain a drug–lipid mixture. An aqueous phase was prepared by dissolving the surfactant in distilled water and heated up to the same temperature of the molten lipid phase. The hot lipid phase was poured onto the hot aqueous phase and homogenization was carried out at 25 000 rpm for 5 min using a Heidolph homogenizer (Heidolph Instruments, Schwabach, Germany). The resultant hot oil-in-water emulsion was sonicated for 30 min (Digital Sonicator; MTI, Michigan, USA). MLX-loaded SLNs were finally obtained by allowing the hot nanoemulsion to cool to room temperature. Blank SLNs were prepared using the same procedure variables.

Meloxicam entrapment efficiency

The entrapment efficiency percentage (EE%), which corresponds to the percentage of MLX encapsulated within the nanoparticles, was determined by measuring the concentration of free MLX in the dispersion medium. The unentrapped MLX percentage was determined by adding 500 µl of MLX-loaded nanoparticles to 9.5 ml of methanol and centrifuging this dispersion at 9000 rpm (Union 32R; Hanil Science Industrial, Gangwondo, Korea) for 30 min. The supernatant was filtered through a Millipore (Sigma-Aldrich, St. Louis, USA) membrane filter (0.2 µm) and analyzed for unencapsulated MLX at 360 nm using a validated UV-spectrophotometric method (model 2401/PC; Shimadzu, Kyoto, Japan) after suitable dilution. The EE% was calculated using the following equation [13]:

$$\mathrm{EE}\,\% = \frac{W_{\text{initial drug}} - W_{\text{free durg}}}{W_{\text{initial drug}}} \times 100,$$

where $W_{\text{initial drug}}$ is the initial mass of the drug used and $W_{\text{free drug}}$ is the mass of the free drug detected in the supernatant after centrifugation of the aqueous dispersion.

Particle size analysis

Particle size analysis of MLX-loaded nanoparticles was performed using a laser diffraction (LD) particle size analyzer (Master Sizer X; Malvern Instruments, Worcestershire, UK) at 25°C. The LD data obtained were evaluated using volume distribution as diameter values of 10, 50, and 90% and span values. The diameter values indicate the percentage of particles possessing a diameter equal to or lower than the given value. The span value is a statistical parameter used to evaluate the particle size distribution: lower the span value, narrower is the particle size distribution. It is calculated using the following equation [14]:

$$\mathrm{Span} = \frac{\mathrm{LD}_{90\%} - \mathrm{LD}_{10\%}}{\mathrm{LD}_{50\%}}.$$

Zeta Potential and pH measurement

The ζ potential was measured in folded capillary cells using a Laser Zetameter (Malvern Instruments). Measurements were performed in distilled water adjusted with a solution of 0.1 mmol/l NaCl at 25°C. The ζ potential values were calculated using the Smoluchowski equation.

The pH values of MLX lipid nanoparticles were measured at 25°C using a digital pH meter (Jenway, Staffordshire, UK).

Transmission electron microscopy

Morphological examination of MLX-loaded SLNs was performed using transmission electron microscopy (TEM) (model JEM-1230; Jeol, Tokyo, Japan). One drop of the diluted sample was deposited onto the surface of a carbon-coated copper grid and negatively stained with a drop of 2% (w/w) aqueous solution of phosphotungstic acid for 30 s. Excess staining solution was wiped off with filter paper, leaving a thin aqueous film on the surface. After staining, the samples were allowed to dry at room temperature for 10 min for analysis [15].

Differential scanning calorimetry

Differential scanning calorimetry (DSC) analysis was carried out using a Shimadzu Differential Scanning Calorimeter (DSC-50; Shimadzu). About 10 mg of sample was added into a 40 µl aluminum pan, which was sealed and heated in the range of 30–300°C at a heating rate of 10°C/min. An empty aluminum pan was used as a reference standard. The analysis was carried out under nitrogen purge.

Rheological study

The rheological properties of the prepared lipid nanoparticles were determined using Brookfield's Viscometer (Brookfield LV-DV II + ; Brookfield, Massachusetts, USA). The sample (20 g) was placed in a beaker and allowed to equilibrate for 5 min. The measurements were carried out at ambient temperature using the suitable spindle. The spindle speed rate was increased in ascending order from 1 to 100 rpm and then decreased in descending order from 100 to 1 rpm, with each kept constant for 10 s before a measurement was made.

In-vitro release study

The in-vitro release of MLX was evaluated using the dialysis bag diffusion technique described by Yang *et al.* [16]. The release studies of MLX from SLNs were performed in phosphate buffer (pH 5.5) and methanol (75 : 25). Aqueous nanoparticulate dispersion equivalent to 2 mg of MLX was placed in a cellulose acetate dialysis bag and sealed at both ends. The dialysis bag was immersed in the receptor compartment containing 50 ml of dissolution medium, which was stirred in a water bath shaker at 100 rpm (Memmert GmbH, Schwabach, Germany) and maintained at 32 ± 2°C. The receptor compartment was covered to prevent evaporation of the dissolution medium. A 2 ml sample of the receiver medium was withdrawn at predetermined time intervals (0.5, 1, 2, 3, 4, 5, 6, 8, 24, and 48 h) and replaced by an equivalent volume of fresh medium to maintain constant volume. The samples were analyzed for drug content spectrophotometrically at 360.5 nm. The data were analyzed using linear regression equations, and the order of drug release from the different formulations was determined.

Statistical analysis

All experiments were repeated three times, and data were expressed as mean value ± SD. The statistical analysis was carried out using one-way analysis of variance. A P value of less than 0.05 was considered statistically significant.

Results and discussion

Preparation of solid lipid nanoparticles

In the present study, MLX-loaded SLNs dispersions were composed of Geleol, Compritol 888 ATO, or Precirol ATO5 as core matrices used in different concentrations of 5, 7.5, and 10% (w/w). These lipid-based carrier systems were stabilized using 0.5, 1, 2.5, and 5% (w/w) Tween 80 or Cremophor RH40. MLX was incorporated at a constant concentration of 0.5% (w/w). The w/w percentage composition of the investigated MLX SLNs is shown in Tables 1 and 2.

Meloxicam entrapment efficiency

The entrapment efficiencies of all SLN formulations are presented in Tables 1 and 2. The entrapment efficiencies varied from 50.42 ± 2.07 to 84.38 ± 0.65%. It can be observed that increasing the amount of surfactant from 0.5 to 1 to 2.5 to 5% (w/w) at a constant amount of lipid (5% w/w) resulted in a gradual significant decrease ($P < 0.05$) in the entrapment efficiencies. However, no change in EE% was observed (Table 1) for Compritol (SLN7 and SLN8) and Precirol SLNs (SLN13 and SLN14) on increasing the Tween 80 concentration from 0.5 to 1%. Moreover, for Geleol SLNs (SLN3 and SLN4), no significant decrease in EE% was observed on increasing the Tween 80 concentration above 2.5% (w/w) ($P > 0.05$). Table 2 shows that using Cremophor RH40 resulted in the same gradual decrease in EE% ($P < 0.05$); however, in case of Geleol SLNs (SLN21 and SLN22) and Precirol SLNs (SLN33 and SLN34), a further increase in the Cremophor RH40 concentration from 2.5 to 5% did not result in significant changes in EE% ($P > 0.05$). This observed decrease in EE% could be

Table 1 Composition and entrapment efficiency of meloxicam solid lipid nanoparticles (%w/w) of different lipids using Tween 80

	Lipid			
Formulas	Type	Concentration	Tween 80 (%)	Entrapment efficiency %[a]
SLN1	Geleol	5	0.5	59.78 ± 1.04
SLN2			1	56.63 ± 0.88
SLN3			2.5	51.03 ± 0.96
SLN4			5	50.42 ± 2.07
SLN5		7.5	0.5	62.30 ± 0.23
SLN6		10		67.49 ± 1.27
SLN7	Compritol	5	0.5	62.47 ± 0.25
SLN8			1	62.22 ± 1.03
SLN9			2.5	57.31 ± 1.92
SLN10			5	54.79 ± 0.21
SLN11		7.5	0.5	65.76 ± 1.77
SLN12		10		72.63 ± 1.66
SLN13	Precirol	5	0.5	65.68 ± 0.09
SLN14			1	65.53 ± 0.40
SLN15			2.5	62.00 ± 0.39
SLN16			5	58.51 ± 0.71
SLN17		7.5	0.5	70.02 ± 0.89
SLN18		10		75.99 ± 3.36

SLN, solid lipid nanoparticle.
[a]Values represent mean ± SD.

Table 2 Composition and entrapment efficiency of meloxicam solid lipid nanoparticles (%w/w) of different lipids using Cremophor RH40

	Lipid			
Formulas	Type	Concentration (%)	Cremophor RH40 (%)	Entrapment efficiency %[a]
SLN19	Geleol	5	0.5	63.31 ± 1.11
SLN20			1	58.33 ± 1.42
SLN21			2.5	52.28 ± 1.89
SLN22			5	53.34 ± 1.20
SLN23		7.5	0.5	65.89 ± 0.83
SLN24		10		69.10 ± 0.42
SLN25	Compritol	5	0.5	68.63 ± 0.34
SLN26			1	62.16 ± 1.64
SLN27			2.5	59.34 ± 0.32
SLN28			5	56.64 ± 0.91
SLN29		7.5	0.5	70.41 ± 0.58
SLN30		10		77.47 ± 0.93
SLN31	Precirol	5	0.5	78.77 ± 0.85
SLN32			1	73.33 ± 1.31
SLN33			2.5	67.71 ± 2.76
SLN34			5	66.79 ± 0.92
SLN35		7.5	0.5	79.51 ± 0.24
SLN36		10		84.38 ± 0.65

SLN, solid lipid nanoparticle.
[a]Values represent mean ± SD.

explained by the partition phenomenon. High surfactant levels in the external phase might increase the partition of the drug from the internal to the external phase of the medium. This increased partition is due to the increased solubilization of the drug in the external aqueous phase such that more volumes of the drug can disperse and dissolve in it [17]. However, some cases in which further increase of surfactant concentration did not lead to a significant change in EE% could suggest that an optimum concentration of the surfactant was reached, sufficient to cover the surface of the nanoparticles effectively. The data also clearly showed that the formulations prepared using Cremophor RH40 as a surfactant had higher EE% compared with those prepared using Tween 80. Similar results were reported by Lv *et al.* [18] for penciclovir-loaded SLNs.

The structure of the lipid used has a great influence on the capacity for drug incorporation. Therefore, the effect of lipid type and concentration on the entrapment efficiency of MLX SLNs was also investigated (Tables 1 and 2). Geleol SLNs exhibited the lowest entrapment of MLX when compared with Compritol and Precirol. This can be attributed to the difference in composition and chain length of the three lipids used. The higher drug entrapment efficiency observed with Precirol and Compritol was attributed to the high hydrophobicity due to the long chain fatty acids attached to the triglycerides, resulting in increased accommodation of lipophilic drugs [19].

The results also showed that increasing the lipid concentration from 5 to 7.5 to 10% (w/w) led to a gradual increase in the entrapment efficiency, which was observed for lipids used at constant concentrations of Tween 80 and Cremophor RH40 ($P<0.05$). However, this increase in the entrapment efficiency is not proportional to the increase in lipid content, which can be observed for the three lipids. An exception was observed for SLN31 and SLN35 wherein a significant increase in EE% occurred only on increasing Precirol concentrations from 7.5 to 10% (w/w). A possible explanation for these observations is that the increase in lipid content can afford more space to encapsulate more drug, thus reducing drug partition in the outer phase [18,20]. This may also be due to an increase in the viscosity of the medium, resulting in faster solidification of nanoparticles, which would further prevent drug diffusion to the external phase of the medium [21].

Particle size analysis

The LD 90% of the formulated SLNs is presented in Table 3. In case of Tween 80 and Cremophor RH40, the nanoparticulate dispersions showed sizes ranging from 210 ± 35.36 to 740 ± 14.14 nm and from 235 ± 21.21 to 730 ± 14.14 nm, respectively. The low span values of different formulations indicate a narrow particle size distribution. The results clearly showed that there was a gradual decrease in particle size with an increase in surfactant concentration from 0.5 to 1 to 2.5 to 5% (w/w) ($P<0.05$). This was observed for all formulations except for SLN1 and SLN2 and for SLN19 and SLN20, in which an initial increase in surfactant concentration from 0.5 to 1% did not lead to a significant decrease in particle size ($P>0.05$). However, a further increase in surfactant concentration above 2.5% for SLN33 and SLN34 did not result in a significant change in particle size ($P>0.05$). The decrease in size of nanoparticles at high surfactant concentrations might be due to an effective reduction in the interfacial tension between the aqueous and lipid phases, leading to the formation of emulsion droplets of smaller sizes [22]. Higher surfactant concentrations effectively stabilize the particles by forming a steric barrier on the particle surface and thereby protect smaller particles and prevent their coalescence into bigger ones [17]. For the formulations in which further increase of surfactant concentration above 2.5% did not reduce the particle size significantly, the data clearly suggest that an optimum concentration of the surfactant was reached,

Table 3 Particle size, ζ potential, and pH values of meloxicam solid lipid nanoparticles

Formulas	LD 90%	Span	ζ potential (mV)	pH	Formulas	LD 90%	Span	ζ potential (mV)	pH
SLN1	420 ± 14.14	0.51	− 15.9	6.15 ± 0.03	SLN19	425 ± 17.68	1.39	− 15.8	5.97 ± 0.01
SLN2	385 ± 7.07	0.63	− 16.0	5.68 ± 0.04	SLN20	370 ± 14.14	1.23	− 17.5	5.82 ± 0.02
SLN3	250 ± 28.28	0.18	− 17.9	5.61 ± 0.06	SLN21	265 ± 7.07	1.10	− 19.8	5.88 ± 0.05
SLN4	210 ± 35.36	0.34	− 20.9	5.53 ± 0.05	SLN22	235 ± 21.21	1.21	− 19.1	5.93 ± 0.08
SLN5	480 ± 14.14	0.67	− 25.5	5.72 ± 0.16	SLN23	490 ± 28.28	1.61	− 20.5	5.85 ± 0.01
SLN6	555 ± 7.07	1.15	− 25.5	5.80 ± 0.04	SLN24	565 ± 7.07	1.64	− 25.2	5.84 ± 0.07
SLN7	580 ± 14.14	0.80	− 18.8	5.77 ± 0.02	SLN25	565 ± 3.54	1.64	− 15.9	5.87 ± 0.01
SLN8	545 ± 7.07	1.27	− 21.1	6.26 ± 0.10	SLN26	505 ± 7.07	1.84	− 17.8	5.71 ± 0.03
SLN9	440 ± 28.28	1.06	− 21.0	5.96 ± 0.08	SLN27	465 ± 21.21	1.72	− 21.6	6.08 ± 0.02
SLN10	385 ± 7.07	0.80	− 22.3	6.09 ± 0.01	SLN28	390 ± 14.14	1.30	− 21.7	5.95 ± 0.07
SLN11	680 ± 28.28	1.28	− 23.0	5.56 ± 0.01	SLN29	685 ± 10.61	1.90	− 19.8	5.92 ± 0.01
SLN12	740 ± 14.14	1.27	− 27.1	5.67 ± 0.08	SLN30	730 ± 14.14	1.95	− 22.8	5.53 ± 0.02
SLN13	470 ± 14.14	0.88	− 16.9	5.91 ± 0.01	SLN31	490 ± 14.14	1.36	− 20.2	6.24 ± 0.08
SLN14	415 ± 21.21	0.83	− 15.7	6.42 ± 0.04	SLN32	435 ± 3.54	1.55	− 20.0	5.26 ± 0.03
SLN15	310 ± 14.14	0.81	− 18.6	5.70 ± 0.05	SLN33	315 ± 7.07	1.29	− 21.4	5.63 ± 0.02
SLN16	265 ± 7.07	0.48	− 22.4	5.70 ± 0.03	SLN34	285 ± 21.21	1.27	− 22.6	5.94 ± 0.03
SLN17	570 ± 28.28	1.03	− 29.8	5.76 ± 0.06	SLN35	580 ± 28.28	1.30	− 20.4	5.56 ± 0.13
SLN18	685 ± 7.07	1.34	− 30.5	5.49 ± 0.08	SLN36	685 ± 7.07	1.71	− 24.3	5.48 ± 0.28

LD, laser diffraction; SLN, solid lipid nanoparticle.

sufficient to cover the surface of nanoparticles effectively and prevent agglomeration during the homogenization process [23].

The results also showed that increasing the lipid content from 5 to 7.5 to 10% (w/w) led to a subsequent increase in particle size (Table 3). Statistical analysis of the data showed no significant increase in particle size in case of SLN19 and SLN23 on increasing the lipid concentration from 5 to 7.5%. A similar result was obtained on increasing the lipid concentration from 7.5 to 10% in case of SLN11 and SLN12 and in SLN29 and SLN30. This increase in particle size may partially be related to the viscosity of the samples, as viscosity is a key factor affecting the ability to create a fine dispersion. At higher lipid contents, the efficiency of homogenization decreases because of a higher viscosity of the sample, resulting in larger particles. Moreover, a high particle concentration at high lipid contents increases the probability of particle contact and subsequent aggregation [24]. The LD 90% values of MLX SLNs of different lipids at a constant surfactant concentration (0.5% w/w) are shown in Fig. 1. For both surfactants used, Compritol showed the largest particle sizes, followed by Precirol and then Geleol. These differences in sizes may be due to differences in the chain lengths and viscosities of the lipids used [25]. Compritol 888 ATO (m.p. 69.0–74.0°C) is a solid lipid based on glycerol esters of behenic acid (C22), in which the main fatty acid is behenic acid (> 85%) but other fatty acids (C16–C20) are also present. Precirol ATO5 (m.p. 50.0–60.0°C) and Geleol (m.p. 54.5–58.4°C) are composed mainly of palmitic (C16) and stearic acids (C18) (> 90%). A high melting temperature resulting in higher viscosity and the long hydrocarbon chain length of Compritol might result in larger particle sizes in comparison with Precirol and Geleol.

Figure 1

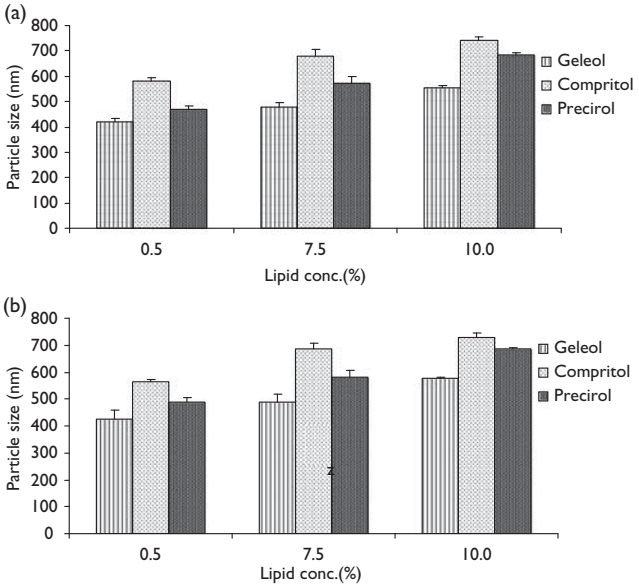

Effect of lipid concentration and type on particle size measured by laser diffraction 90% of meloxicam solid lipid nanoparticles using (a) Tween 80 and (b) Cremophor RH40.

ζ Potential analysis and pH measurements

As shown in Table 3, all formulations were negatively charged; the ζ potential varied from − 15.7 mV (SLN14) to − 30.5 mV (SLN18), indicating relatively good stability and dispersion quality. It was noticeable that as the amount of surfactant increased in the formulation the ζ potential became more negative. However, the influence of surfactant type is less pronounced.

Tween 80 and Cremophor RH40 being nonionic surfactants could successfully be used in the production of relatively stable dispersions. This behavior could be a result of the strong effect of surfactants in an emulsion system on the adsorbed layer thickness [26]. Although nonionic surfactants could not ionize into charged groups like ionic ones, they still demonstrated an effect on the ζ potential. This might be due to molecular polarization and adsorption of emulsifier molecules onto the charge in water: they were absorbed onto the emulsifier layer of the

particle/water interface, and an electric double layer similar to an ionic layer was formed. Considering the effect of lipid type and concentration on the ζ potential of the produced SLN formulations, the results showed no direct relationship between the type of lipid used and the measured ζ values. In contrast, as the lipid concentration increased, the ζ potential was found to become more negative. Rahman *et al.* [17] reported the same observation when studying the effect of increasing Compritol concentrations in the final formulation.

The bulk pH values of the stratum corneum and upper viable epidermis have been measured to be 4.0–4.5 and 5.0–7.0, respectively [27]. For a topical preparation to be applied safely onto the skin, its pH should lie within this range. The pH values of different MLX SLN formulations ranged from 5.26 ± 0.03 to 6.42 ± 0.04 (Table 3) and hence were in the required range.

Transmission electron microscopy

TEM was used to investigate the morphology of MLX-loaded SLNs. It was evident from the TEM images that the nanoparticles were almost spherical with smooth morphology, appeared as black dots, and were well dispersed and separated on the surface (Fig. 2). This description is in agreement with a previous observation that the use of chemically heterogeneous lipids in combination with heterogeneous surfactants favors the formation of ideally spherical lipid nanoparticles [11]. The figure illustrates the presence of a very thin layer surrounding the particles, which suggests a drug-enriched core model. This model can be achieved if during the lipid solidification process, the drug precipitates first, which results in a drug-enriched core covered with a lipid shell that has a lower drug concentration. This drug distribution within the nanoparticles will have its impact on the in-vitro drug release profile discussed.

Differential scanning calorimetry analysis

Figure 3 shows the DSC thermograms of pure MLX, bulk lipids (Geleol, Compritol 888 ATO, and Precirol ATO5), and MLX-loaded SLNs. Pure MLX showed a sharp endothermic peak at 259.54°C, corresponding to its melting point, indicating its characteristic crystalline nature. Bulk Geleol showed a distinctive melting peak at 66.01°C, whereas Compritol 888 ATO showed a sharp peak at 74.22°C. The bulk Precirol ATO5 exhibits a sharp endothermic event, ascribing to melting, around 63.35°C, with a small but well-defined shoulder at 57.37°C, which might be due to melting of the α-polymorphic form [28]. These sharp melting endothermic peaks of bulk lipids indicate that the starting materials were crystalline. As observed in Fig. 3, the thermograms of all investigated SLN systems did not show the melting peak of MLX, indicating the conversion of crystalline MLX to the amorphous form, which could be attributed to complete dissolution of the drug in the molten lipid matrix. The melting points of Geleol, Compritol 888 ATO, and Precirol ATO5 in the SLN form were depressed, showing a slight shift toward the lower temperatures when compared with the corresponding bulk lipids. This

Figure 2

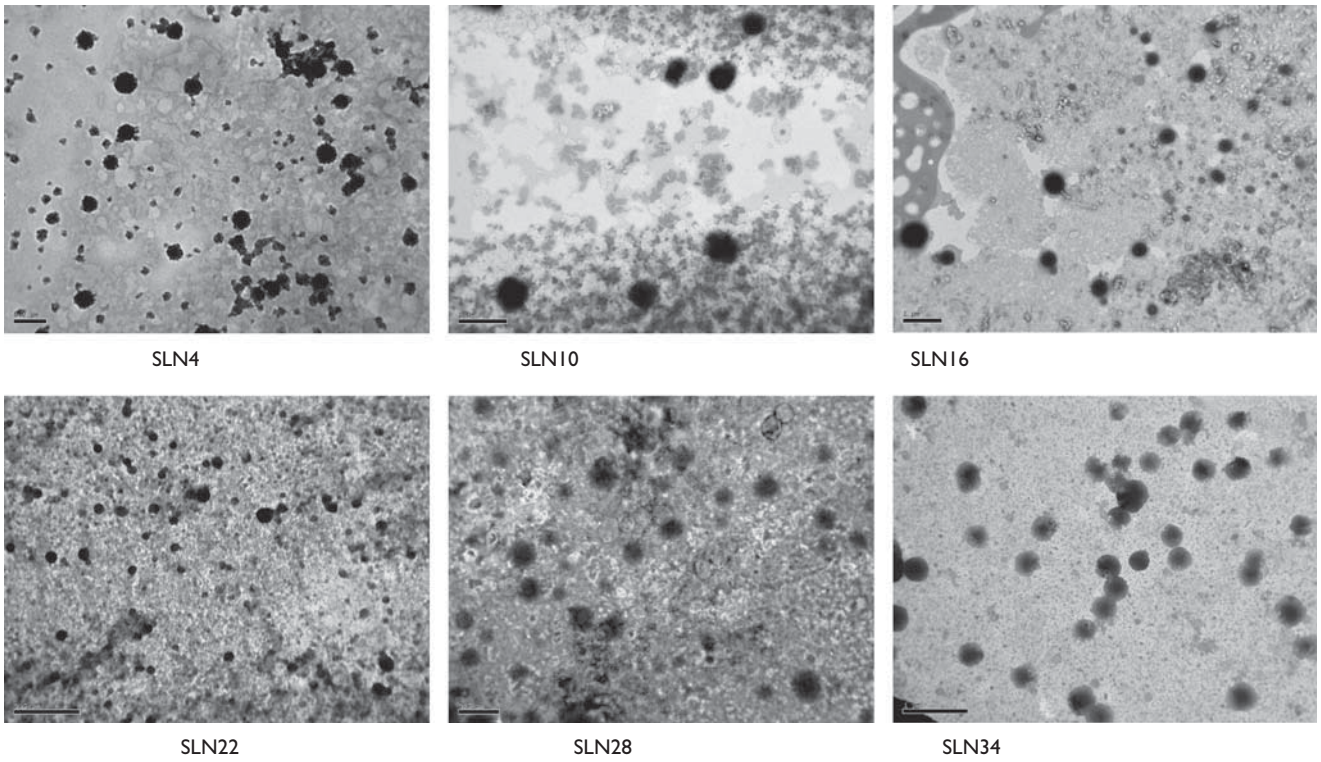

Transmission electron micrographs of meloxicam solid lipid nanoparticles.

Figure 3

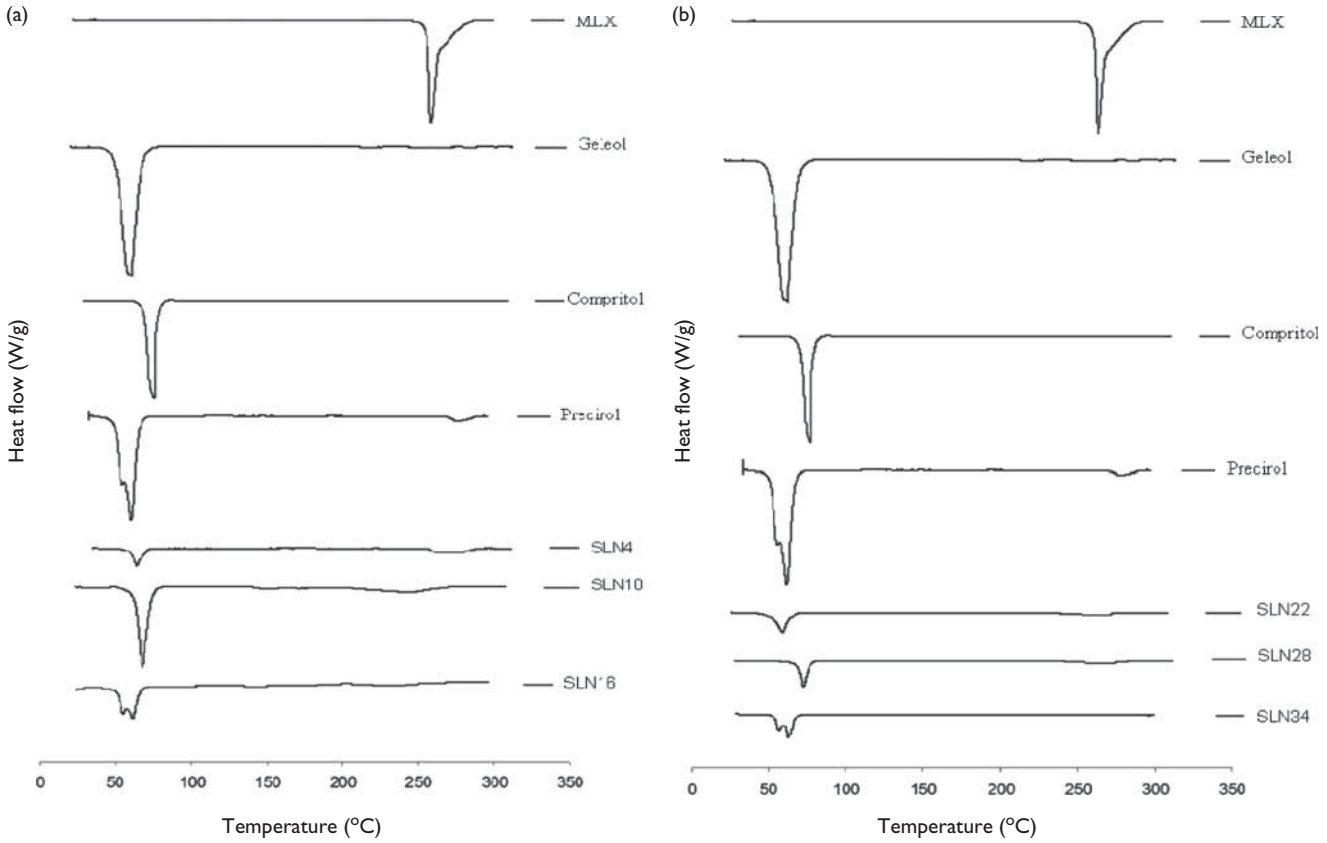

Differential scanning calorimetry thermograms of pure meloxicam (MLX), bulk lipids (Geleol, Compritol, and Precirol), and MLX solid lipid nanoparticles (SLNs) using. (a) Tween 80 and (b) Cremophor RH40.

melting point depression could be due to the small particle size (nanometer range), the high specific surface area, and the presence of a surfactant. In other words, the depression can be attributed to the Kelvin effect [4]. Kelvin realized that small, isolated particles would melt at a temperature lower than the melting temperature of bulk materials. In the same way, the melting enthalpy values of different lipids in SLN formulations showed drastic depression compared with those of their bulk lipids. These lower melting enthalpy values should suggest a less-ordered lattice arrangement of the lipid within the nanoparticles compared with those of the bulk materials [13]. For the less-ordered crystalline or amorphous state, the melting of the substance requires less energy compared with the perfectly crystalline substance, which needs to overcome the lattice force.

Rheological study

The rheological properties of MLX SLNs were presented by plotting the shear stress (SS) versus the shear rate (SR) (flow curves) and the viscosity versus the shear rate (viscosity curves) curves [29,30]. The rheograms of selected different SLN formulations are shown in Fig. 4. As shown from the continuous shear rheometry, SLN dispersions revealed a non-Newtonian flow. The viscosity of non-Newtonian fluids changes according to the shear rate, that is, has no constant viscosity [31]. This flow was characterized by the shear-thinning behavior, in which the viscosity of the SLN dispersions decreased with an increase in the shear rate. At present, shear-thinning materials are also considered thixotropic, because it always takes time, even though limited, to regroup the microstructural elements [32]. In addition, the type of lipid affected the viscosity of the final product. For both surfactants used, Geleol SLNs showed lower viscosities compared with Precirol and Compritol SLNs.

In-vitro release studies

To compare the drug release profile from the prepared SLN formulations, the release efficiency (RE%) after 48 h was used. The data clearly showed that the release of the drug from the investigated SLN formulations can be influenced by the type and concentration of the surfactant, in addition to the nature and concentration of lipid matrix used. Some formulations of Tween 80 and Cremophor RH40 SLNs were selected, representing those of highest and lowest surfactant and lipid concentrations. The selected formulations of Tween 80 SLNs were SLN1, SLN4, SLN6, SLN7, SLN10, SLN12, SLN13, SLN16, and SLN18, whereas those of Cremophor RH40 SLNs were SLN19, SLN22, SLN24, SLN25, SLN28, SLN30, SLN31, SLN34, and SLN36. The percentage of MLX released during ~48 h ranged from

Figure 4

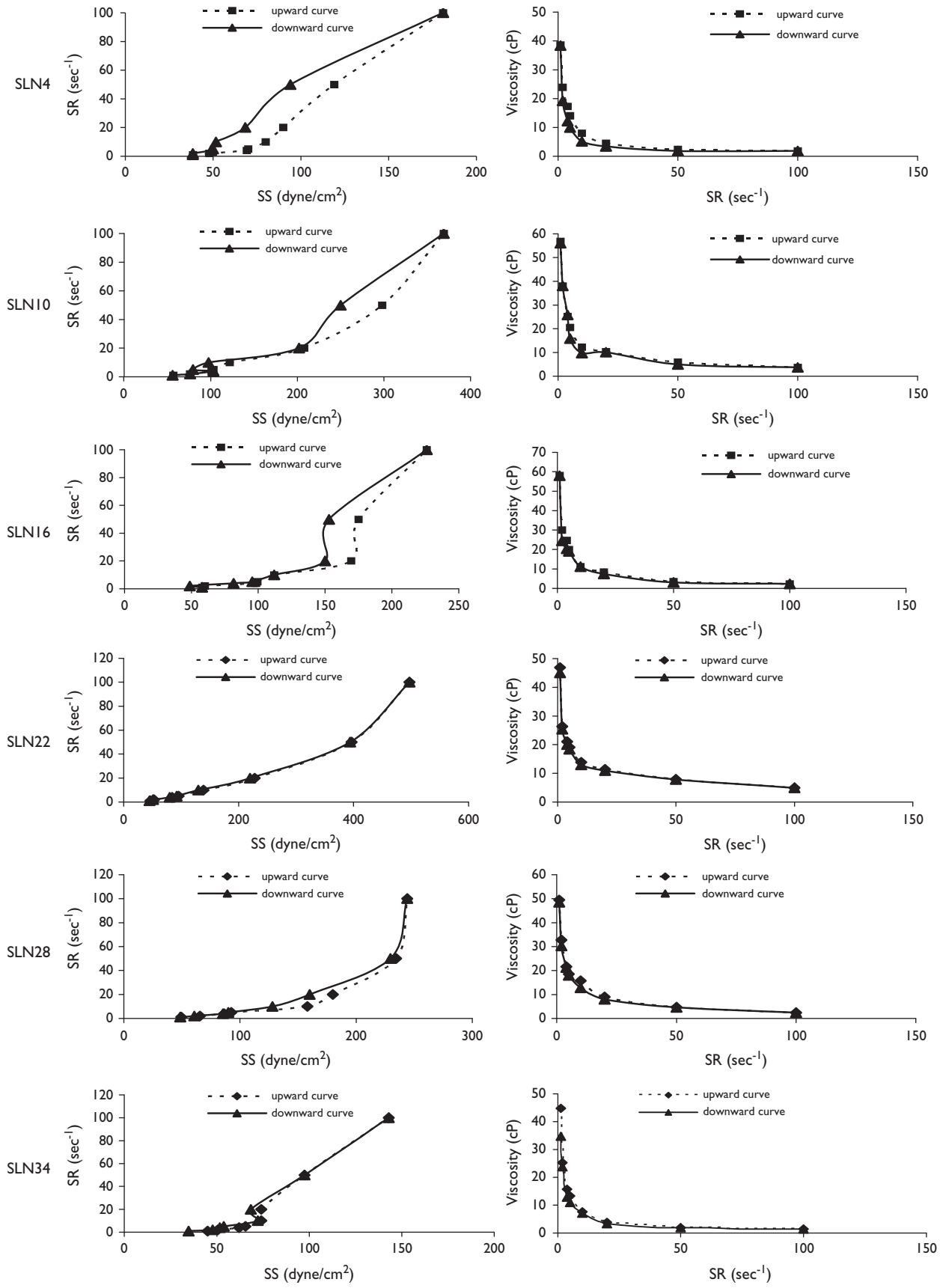

Rheograms of meloxicam solid lipid nanoparticles (SLNs). SR, shear rate; SS, shear stress.

29.42 (SLN18) to 76.61% (SLN4) in case of Tween 80 SLNs and from 29.33 (SLN31) to 72.72% (SLN28) in case of Cremophor RH40 SLNs (Fig. 5). Interestingly, the amount of surfactant used had a great influence on the release pattern of SLNs. Increasing the surfactant concentration from 0.5 to 5% (w/w) led to an increase in the percentage of MLX released and the RE% ($P<0.05$) (Fig. 5 and Table 4).

The fast or rapid release and higher release efficiency observed at higher surfactant concentrations could be explained by the partitioning of the drug between the melted lipid phase and aqueous surfactant phase during particle production. During particle production by the hot homogenization technique, the drug partitions from the liquid oil phase to the aqueous water phase. The amount of drug partitioning to the water phase will increase with the increase of drug solubility in the water phase as a result of increasing the temperature of the aqueous phase and surfactant concentration. Higher the temperature and surfactant concentrations, greater is the solubility of the drug in the water phase. During cooling of the produced O/W nanoemulsion, the solubility of the drug in the water phase decreases continuously with decrease in the temperature of the water phase, which implies a repartitioning of the drug into the lipid phase. When reaching the recrystallization temperature of the lipid, a solid lipid core starts forming, including the drug that is present at this temperature in this lipid phase. Reducing the temperature of the dispersion further increases the pressure on the drug because of its reduced solubility in water to further repartition into the lipid phase. The already crystallized core is not accessible anymore for the drug; consequently, the drug concentrates in the still liquid outer shell of the SLN and/or on the surface of the particles. The amount of drug in the outer shell is released relatively rapidly, whereas the drug incorporated into the particle core is released gradually [33].

Figure 5

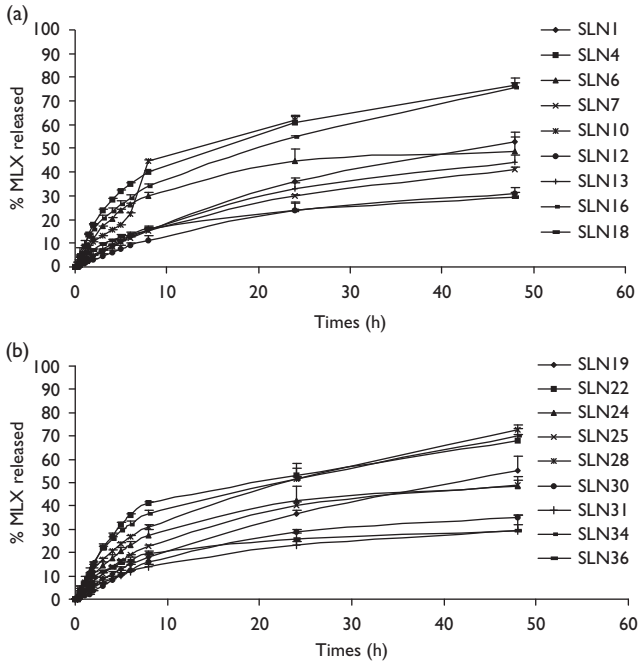

The release profile of meloxicam (MLX) from solid lipid nanoparticles (SLNs) using (a) Tween 80 and (b) Cremophor RH40 as surfactants.

Table 4 Release efficiency and $t_{50\%}$ (h) of the selected meloxicam solid lipid nanoparticles formulations

Surfactants					
Tween 80			Cremophor RH40		
Formulas[a]	RE 48 (%)	$t_{50\%}$ (h)	Formula[a]	RE 48 (%)	$t_{50\%}$ (h)
SLN1	32.42 ± 1.28	33.72	SLN19	33.74 ± 2.50	33.10
SLN4	55.55 ± 1.70	18.73	SLN22	50.18 ± 1.70	23.28
SLN6	38.93 ± 4.37	43.46	SLN24	37.08 ± 4.31	44.17
SLN7	26.62 ± 0.72	56.19	SLN25	34.97 ± 0.89	39.39
SLN10	39.98 ± 1.82	25.12	SLN28	48.00 ± 0.88	20.65
SLN12	20.58 ± 1.98	92.44	SLN30	24.67 ± 1.52	68.74
SLN13	29.05 ± 1.77	47.14	SLN31	20.78 ± 1.51	117.54
SLN16	51.08 ± 0.77	20.14	SLN34	48.95 ± 3.49	24.03
SLN18	21.58 ± 2.57	132.75	SLN36	23.35 ± 3.23	45.501

RE, release efficiency; SLN, solid lipid nanoparticle; $t_{50\%}$ (h), time required to release 50% of the drug.
[a]See Tables 1 and 2 for the description of the formulations.

As regards the type of lipid matrix, the results clearly showed that among the glycerides used, the highest release was achieved with Geleol when compared with Compritol and Precirol. Being the lipid of highest monoglyceride content, Geleol showed the highest release efficiency and consequently lower $t_{50\%}$. In case of Compritol and Precirol, the relatively slow release and higher $t_{50\%}$ can be attributed to the hydrophobic long chain fatty acids of the triglycerides that retain the lipophilic drug, resulting in a more sustained release [23,34]. This effect was evident in Tween 80 SLN formulations, whereas in case of Cremophor RH40 SLNs the difference between the three lipids was less pronounced (Fig. 5 and Table 4).

The results also indicate the effect of lipid concentration on SLNs' release profile: increasing the lipid concentration from 5 to 10% (w/w) resulted in a corresponding decrease in the percentage of MLX released and a consequent increase in $t_{50\%}$ for Tween 80 and Cremophor RH40 SLNs (Fig. 5 and Table 4). However, in case of Geleol SLNs (SLN1, SLN6, SLN19, and SLN24), a slight increase in RE% was observed (Table 4). This observed decrease in the release profile can be attributed to the higher lipid content encapsulating the drug, thus reducing drug partition in the outer phase and consequently its release in the receiver media. The release profiles of these SLNs resemble the drug-enriched core model [35]. In such a model, the drug-enriched core is surrounded by a practically drug-free lipid shell. Because of the increased diffusional distance and hindering effects by the surrounding solid lipid shell, the drug has a sustained release profile.

The release pattern of the drug from all SLN formulations followed the Higuchi's equation. The R^2 values

ranged from 0.9151 to 0.9977 in case of Tween 80 and from 0.9115 to 0.9984 in case of Cremophor RH40. This result is generally in agreement with many studies that reported that drug-loaded SLNs provide a controlled release pattern following Higuchi's square root model [36,37].

Conclusion

In this study, the MLX-loaded SLNs were successfully prepared using modified high-shear homogenization and ultrasound techniques. Physicochemical characterization revealed that the prepared drug-loaded SLNs were of spherical shape and homogenously distributed. The DSC analysis showed the amorphous state of MLX in SLNs. SLNs achieved high drug incorporation with small-sized particles (nanosize) and showed shear-thinning rheological behavior. The in-vitro release behavior was greatly affected and can be controlled by optimizing the compositional variables. The sustained release behavior of MLX-loaded SLNs together with the favorable physicochemical characteristics supports that SLNs are promising delivery systems for poorly water-soluble drugs such as MLX and can form a foundation for further clinical studies for the topical delivery of MLX.

Acknowledgements

Conflicts of interest

There are no conflicts of interest.

References

1 Sarathchandiran I. A review on nanotechnology in solid lipid nanoparticles. Int J Pharm Develop Technol 2012; 2:45–61.

2 Fang J-Y, Fang C-L, Liu C-H, Su Y-H. Lipid nanoparticles as vehicles for topical psoralen delivery: solid lipid nanoparticles (SLN) versus nanostructured lipid carriers (NLC). Eur J Pharmaceut Biopharmaceut 2008; 70:633–640.

3 Mei Z, Chen H, Weng T, Yang Y, Yang X. Solid lipid nanoparticle and microemulsion for topical delivery of triptolide. Eur J Pharmaceut Biopharmaceut 2003; 56:189–196.

4 Jenning V, Gysler A, Schäfer-Korting M, Gohla SH. Vitamin A loaded solid lipid nanoparticles for topical use: occlusive properties and drug targeting to the upper skin. Eur J Pharmaceut Biopharmaceut 2000; 49:211–218.

5 Sharma A, Jindal M, Aggarwal G, Jain S. Development of a novel method for fabrication of solid lipid nanoparticles: using high shear homogenization and ultrasonication. Res J Pharm Biol Chem Sci 2010; 1:265–274.

6 Chen H, Chang X, Du D, Liu W, Liu J, Weng T, *et al*. Podophyllotoxin-loaded solid lipid nanoparticles for epidermal targeting. J Controll Release 2006; 110:296–306.

7 Sivaramakrishnan R, Nakamura C, Mehnert W, Korting HC, Kramer KD, Schäfer-Korting M. Glucocorticoid entrapment into lipid carriers – characterisation by parelectric spectroscopy and influence on dermal uptake. J Controll Release 2004; 97:493–502.

8 Engelhardt G. Pharmacology of meloxicam, a new non-steroidal anti-inflammatory drug with an improved safety profile through preferential inhibition of COX-2. Br J Rheumatol 1996; 35 (Suppl 1):4–12.

9 Kaplan-Machlis B, Klostermeyer BS. The cyclooxygenase-2 inhibitors: safety and effectiveness. Ann Pharmacother 1999; 33:979–988.

10 Pairet M, Van Ryn J, Schierok H, Mauz A, Trummlitz G, Engelhardt G. Differential inhibition of cyclooxygenases-1 and -2 by meloxicam and its 4′-isomer. Inflamm Res 1998; 47:270–276.

11 Mehnert W, Mäder K. Solid lipid nanoparticles: production, characterization and applications. Adv Drug Deliv Rev 2001; 47 (2–3):165–196.

12 Venkateswarlu V, Manjunath K. Preparation, characterization and in vitro release kinetics of clozapine solid lipid nanoparticles. J Controll Rel 2004; 95:627–638.

13 Hou D, Xie C, Huang K, Zhu C. The production and characteristics of solid lipid nanoparticles (SLNs). Biomaterials 2003; 24:1781–1785.

14 Teeranachaideekul V, Souto EB, Junyaprasert VB, Müller RH. Cetyl palmitate-based NLC for topical delivery of coenzyme Q10 – development, physicochemical characterization and in vitro release studies. Eur J Pharmaceut Biopharmaceut 2007; 67:141–148.

15 Li Y, Dong L, Jia A, Chang X, Xue H. Preparation and characterization of solid lipid nanoparticles loaded traditional Chinese medicine. Int J Biol Macromol 2006; 38 (3–5):296–299.

16 Yang SC, Lu LF, Cai Y, Zhu JB, Liang BW, Yang CZ. Body distribution in mice of intravenously injected camptothecin solid lipid nanoparticles and targeting effect on brain. J Controll Rel 1999; 59:299–307.

17 Rahman Z, Zidan AS, Khan MA. Non-destructive methods of characterization of risperidone solid lipid nanoparticles. Eur J Pharmaceut Biopharmaceut 2010; 76:127–137.

18 Lv Q, Yu A, Xi Y, Li H, Song Z, Cui J, *et al*. Development and evaluation of penciclovir-loaded solid lipid nanoparticles for topical delivery. Int J Pharm 2009; 372 (1–2):191–198.

19 Jenning V, Gohla SH. Encapsulation of retinoids in solid lipid nanoparticles (SLN). J Microencapsul 2001; 18:149–158.

20 Shah KA, Date AA, Joshi MD, Patravale VB. Solid lipid nanoparticles (SLN) of tretinoin: potential in topical delivery. Int J Pharm 2007; 345 (1–2): 163–171.

21 Yang Y-Y, Chung T-S, Bai X-L, Chan W-K. Effect of preparation conditions on morphology and release profiles of biodegradable polymeric microspheres containing protein fabricated by double-emulsion method. Chem Eng Sci 2000; 55:2223–2236.

22 Liu J, Gong T, Wang C, Zhong Z, Zhang Z. Solid lipid nanoparticles loaded with insulin by sodium cholate-phosphatidylcholine-based mixed micelles: preparation and characterization. Int J Pharm 2007; 340 (1–2):153–162.

23 Kumar VV, Chandrasekar D, Ramakrishna S, Kishan V, Rao YM, Diwan PV. Development and evaluation of nitrendipine loaded solid lipid nanoparticles: Influence of wax and glyceride lipids on plasma pharmacokinetics. Int J Pharm 2007; 335 (1–2):167–175.

24 Freitas C, Müller RH. Effect of light and temperature on zeta potential and physical stability in solid lipid nanoparticle (SLN) dispersions. Int J Pharm 1998; 168:221–229.

25 Ahlin P, Kristl J, Šmid-Korbar J. Optimization of procedure parameters and physical stability of solid lipid nanoparticles in dispersions. Acta Pharm 1998; 48:259–267.

26 Liu F, Yang J, Huang L, Liu D. New cationic lipid formulations for gene transfer. Pharm Res 1996; 13:1856–1860.

27 Plasencia I, Norlén L, Bagatolli LA. Direct visualization of lipid domains in human skin stratum corneum's lipid membranes: effect of pH and temperature. Biophys J 2007; 93:3142–3155.

28 Araújo J, Gonzalez-Mira E, Egea MA, Garcia ML, Souto EB. Optimization and physicochemical characterization of a triamcinolone acetonide-loaded NLC for ocular antiangiogenic applications. Int J Pharm 2010; 393 (1–2):167–175.

29 Illing A, Unruh T. Investigation on the flow behavior of dispersions of solid triglyceride nanoparticles. Int J Pharm 2004; 284 (1–2):123–131.

30 Liu W, Hu M, Liu W, Xue C, Xu H, Yang X. Investigation of the carbopol gel of solid lipid nanoparticles for the transdermal iontophoretic delivery of triamcinolone acetonide acetate. Int J Pharm 2008; 364:135–141.

31 Barnes HA. Thixotropy – a review. J Non-Newtonian Fluid Mech 1997; 70 (1–2):1–33.

32 Lee CH, Moturi V, Lee Y. Thixotropic property in pharmaceutical formulations. J Controll Rel 2009; 136:88–98.

33 Zur Mühlen A, Mehnert W. Drug release and release mechanism of prednisolone loaded solid lipid nanoparticles. Pharmazie 1998; 53: 552–555.

34 Harivardhan Reddy L, Murthy RSR. Etoposide-loaded nanoparticles made from glyceride lipids: formulation, characterization, in vitro drug release, and stability evaluation. AAPS PharmSciTech 2005; 6:E158–E166.

35 Wissing SA, Kayser O, Müller RH. Solid lipid nanoparticles for parenteral drug delivery. Adv Drug Deliv Rev 2004; 56:1257–1272.

36 Tiyaboonchai W, Tungpradit W, Plianbangchang P. Formulation and characterization of curcuminoids loaded solid lipid nanoparticles. Int J Pharm 2007; 337 (1–2):299–306.

37 Vivek K, Reddy H, Murthy RSR. Investigations of the effect of the lipid matrix on drug entrapment, in vitro release, and physical stability of olanzapine-loaded solid lipid nanoparticles. AAPS PharmSciTech 2007; 8:E1–E9.